Published in final edited form as:
Neuroscience. 2014 June 20; 271: 1–8. doi:10.1016/j.neuroscience.2014.04.025.

MRI evaluation of BBB disruption after adjuvant AcSDKP treatment of stroke with tPA in rat

Guangliang Ding, PhD[1], **Zhenggang Zhang, MD, PhD**[1], **Michael Chopp, PhD**[1,2], **Lian Li, PhD**[1], **Li Zhang, MD**[1], **Qingjiang Li, MBA**[1], **Min Wei, BS**[1], and **Quan Jiang, PhD**[1]

[1]Department of Neurology, Henry Ford Hospital, 2799 West Grand Boulevard, Detroit, MI 48202, USA

[2]Department of Physics, Oakland University, Rochester, MI 48309, USA

Abstract

The primary limitation of thrombolytic treatment of ischemic stroke with tPA is the hemorrhagic risk. We tested AcSDKP (N-acetyl-seryl-aspartyl-lysyl-proline), as an auxiliary therapeutic agent, to reduce blood-brain barrier (BBB) disruption in a combination tPA thrombolytic treatment of stroke. Wistar rats subjected to embolic stroke were randomly assigned to either the tPA monotherapy group (n=9) or combination of tPA and AcSDKP treatment group (n=9) initiated at 4h after ischemia. MRI measurements were performed before and after the treatments. Immunohistochemical staining and measurements were performed to confirm MRI findings. Longitudinal MRI permeability measurements with Gd-DTPA demonstrated that combination treatment of acute embolic stroke with AcSDKP and tPA significantly reduced BBB leakage, compared to tPA monotherapy, at 3 and 6 days (18.3±9.8mm^3 vs 65.0±21.0mm^3, $p<0.001$) after onset of stroke, although BBB leakage was comparable between the two groups prior to the treatments (6.8±4.4mm^3 vs 4.3±3.3mm^3, $p>0.18$). The substantial reduction of BBB leakage observed in the combination treatment group was closely associated with reduced ischemic lesions measured by T_2 maps (113.6±24.9mm^3 vs 188.1±60.8mm^3, $p<0.04$ at 6d). Histopathological analysis of the same population rats showed that the combination treatment significantly reduced parenchymal fibrin deposition (0.063±0.059mm^2 vs 0.172±0.103mm^2, $p<0.03$) and infarct volume (146.7±35.9mm^3 vs 199.3±60.4mm^3, $p<0.05$) compared to the tPA monotherapy at 6 days after stroke. MRI provides biological insight into the therapeutic benefit of combination treatment of stroke with tPA and AcSDKP 4 hours after onset, and demonstrates significantly improved cerebrovascular integrity with neuroprotective effects compared with tPA monotherapy.

Please send all correspondence to: Quan Jiang, Ph.D., Henry Ford Hospital, Neurology Department, E&R B126, 2799 West Grand Boulevard, Detroit, MI 48202, 313-916-8735 Telephone, 313-916-1324 Fax, qjiang1@hfhs.org.

Conflict of interest disclosures

All authors have approved the final article. No conflicts are declared for all authors.

Keywords

BBB; stroke; tPA; AcSDKP; MRI; rat

Introduction

Cerebral arterial thrombosis is the predominant cause of ischemia which accounts for more than 80% of stroke cases (Fieschi et al., 1989). The primary limitation of thrombolytic treatment of ischemic stroke with tissue plasminogen activator (tPA) is the risk of hemorrhage (NINDS, 1997). Currently, only a small percentage of patients receive tPA, despite the extension of the treatment window from 3 to 4.5 hours (Hacke et al., 2008). However, in experimental studies, the treatment of embolic stroke with tPA and adjuvant agents, such as statins (Zhang et al., 2012), a proteasome inhibitor (Zhang et al., 2012), or a glycoprotein IIb/IIIa receptor inhibitor (Ding et al., 2005) extend the therapeutic window of thrombolysis without increasing the risk of hemorrhage. These agents also enhance the therapeutic efficacy of tPA (Ding et al., 2005, Zhang et al., 2012). Thus, a proper auxiliary therapeutic agent will reduce hemorrhagic risk, enhance thrombolytic efficacy and extend the therapeutic window in combination treatment of thrombolysis with tPA.

AcSDKP, a tetrapeptide (N-acetyl-seryl-aspartyl-lysyl-proline), exhibits cytokine characteristics (Yang et al., 2004), although it is usually not classified as such due to its small size. Containing anti-inflammation, anti-fibrotic and angiogenic properties, AcSDKP, therefore, is a potential adjunctive candidate for thrombolysis with tPA. AcSDKP is primarily a potent natural inhibitor of hematopoietic stem cell proliferation (Jackson et al., 2000). However, AcSDKP also inhibits collagen production by cardiac fibroblasts in vitro (Zhuo et al., 2007); while in vivo it blocks collagen deposition in the left cardiac ventricle in rats with hypertension or myocardial infarction (Rasoul et al., 2004), and it reverses inflammation and fibrosis in rats with heart failure after myocardial infarction (Yang et al., 2004). AcSDKP also acts as a mediator of angiogenesis; it stimulates in vitro migration and differentiation of endothelial cells into capillary-like structures, induces the formation of blood vessels (Liu et al., 2003), and increases capillary density in rat heart with myocardial infarction (Wang et al., 2004).

We have demonstrated that the combination thrombolytic therapy of embolic stroke with tPA and AcSDKP is neuroprotective and effective in maintaining cerebral microvascular patency and integrity (Zhang et al., 2014). In the present study, we focused on the evolution of the disruption of the blood-brain barrier (BBB) after stroke in rats treated with tPA alone or combination of tPA and AcSDKP. In order to compare BBB integrity before and after receiving the thrombolytic treatments for each animal, magnetic resonance imaging (MRI) was employed to non-invasively evaluate the status of BBB disruption.

Experimental Procedures

All experimental procedures were conducted and performed in accordance with guidelines for animal research under a protocol approved by the Institutional Animal Care and Use

Committee of Henry Ford Hospital. MRI scan and data analysis, embolic stroke surgery and tPA treatments, and histological measurements, were performed in a double-blind fashion.

1. Animal Model and Experimental Protocol

Adult male Wistar rats (Jackson Laboratory, Bar Harbor, ME) 8–12 weeks of age and weighing 300 to 350g were subjected to embolic stroke. This model of embolic stroke provides a reproducible infarct volume localized to the territory supplied by the middle cerebral artery (MCA) (Zhang et al., 1997). Briefly, an aged white clot (blood of a rat was withdrawn into 20cm PE-50 tubing), which was prepared 24 hours (retained at 25°C for 2h and at 4°C for 22h) before stroke surgery, was slowly injected into the internal carotid artery to the origin of the MCA. The stroke rats were randomly assigned to either the tPA alone treatment (monotherapy) group (n=9), or tPA and AcSDKP treatment (combination) group (n=9).

In the monotherapy group, recombinant human tPA (Genentech, San Francisco, CA) was administered intravenously at a dose of 10mg/kg, 10% bolus at 4h after ischemia, and the remainder as a continuous infusion with a syringe infusion pump (Harvard Apparatus, South Natick, MA) over a 30 minute interval. Because the sensitivity of the rat to the recombinant human tPA is 10 times lower than in the human, dose of tPA received by rats (10mg/kg) in this experiment is 10 times higher than that used in clinic (1mg/kg) (Haelewyn et al., 2010). The selected dose of tPA has been previously shown to be effective for this model (Zhang et al., 1997). In addition to being administered the same protocol of tPA, the combination group received AcSDKP at a dose of 0.4mg/kg subcutaneously infused using an osmotic pump (Alzet, Cupertino, CA) from 4 to 72h after embolic MCA occlusion (MCAo). For the monotherapy group, rats received the same fluid volume of saline subcutaneously infused using the osmotic pump.

MRI was performed prior to MCAo surgery, as an internal control. MRI then was performed immediately post MCAo, and at 72h and 144h after MCAo for all rats. All animals were euthanized 6d post stroke after completing the last MRI scan.

2. MRI measurements

MRI was performed using a Varian 7T system (Varian Inc, Palo Alto, CA) with Bruker birdcage transmitter and surface receiver coils (Bruker Company, Billerica, MA). During MRI measurements, the anesthesia was maintained using a gas mixture of N_2O (70%), O_2 (30%), and isoflurane (1.00–1.50%) with a flow 1.0L/min, and stereotaxic ear bars were utilized to minimize 7 movement. Rectal temperature was kept at 37°C±1.0°C using a feedback controlled air heater. A fast gradient echo imaging sequence was used for reproducible positioning of the animal in the magnet at each MRI session. MRI sequences included T_2-weighted imaging (T2WI), diffusionweighted imaging (DWI) and Look-Locker (L-L) sequence of T_1 measurement for a quantitative permeability related parameter of blood-to-brain transfer rate constant (K_i) of gadoliniumdiethylenetriamine penta-acetic acid (Gd-DTPA, magnevist®, Berlex Inc, Montville, NJ). Contrast enhanced T_1-weighted imaging (CE-T1WI) was composed of pre- and post-injection of Gd-DTPA. The parameters for these pulse sequences were previously described (Ding et al., 2005, Ding et al., 2006).

3. Immunohistochemical staining

Rats were anesthetized with intraperitoneal injection with chloral hydrate, and were perfused transcardially with saline, followed by 4% paraformaldehyde. Brains were isolated, post-fixed in 4% paraformaldehyde for 2 days at room temperature, and then processed for paraffin sectioning. Coronal sections (6μm thick) were cut from each block and stained with hematoxylin and eosin (H&E) for the evaluation of ischemic lesion and blood red cells in cerebral parenchymal tissue using light microscopy. A goat anti-mouse fibrinogen/fibrin antibody was used at a titer of 1:1000 to assess the deposition of fibrin and fibrinogen-related antigen in brain (Accurate Chemical & Scientific, Westbury, NY). Although this antibody detects both fibrin and fibrinogen, the titer of the antibody used in the present study primarily reacted with fibrin.

4. Data and Statistical Analysis

MRI image analysis was generally performed with homemade software, Eigentool (Ding et al., 2005, Ding et al., 2006). All two-dimensional (T1WI, T2WI, DWI, L-L) images were reconstructed using a 128 × 128 matrix. The T_2, apparent diffusion coefficient (ADC) of water or T_1 maps were obtained from T2WI, DWI or L-L images, respectively, using a linear leastsquares fit to the plot of the natural logarithm. The MicroComputer Imaging Device (MCID) system (Imaging Research Inc, Ontario, Canada) was used for immunohistochemical measurements. H&E and fibrin stained sections were evaluated at 10×, or 40× magnifications, respectively. The positive reaction areas were measured by tracing the areas above the threshold for each stained section on the computer monitor screen.

Ischemic lesion volumes of MRI were measured on ADC maps immediately after MCAo, and on T_2 maps for the remaining times (3 and 6 days post MCAo) (Ding et al., 2005). The mean plus two times standard deviation (SD) of the contralateral measurements on the K_i map was used as a threshold to identify region-of-interest (ROI) with elevated K_i values, and the size and mean value of the ROI on the K_i map were collected. The same measurement was performed on the subtraction image of pre-Gd T1WI from post-Gd T1WI. Referring to the image intensity of the pre-Gd T1WI, the percentage of image intensity increase was measured.

Analysis of variance (ANOVA) was performed. The effect was detected at the 0.05 level. Pearson's correlation analysis and normal t-test were applied for MRI and histological measurements. MRI and histological measurements are summarized as mean and standard deviation.

Results

The typical evolution patterns of MRI permeability, K_i, at 1, 72 and 144 hours after stroke are demonstrated in figure 1 for representative rats with combination treatment of tPA and AcSDKP (upper row) or with tPA monotherapy (lower row), respectively. The cerebral tissue volumes with elevated permeability values, which were employed to evaluate the BBB disruption, increased more slowly in the combination treated rats than in monotherapy rats. The quantitative K_i measurements, as shown in Table 1 and Fig.2a, demonstrated that

the volumes of elevated permeability were not significantly different at 1h (6.8±4.4mm^3 for the combination group vs 4.3±3.3mm^3 for the monotherapy group, $p>0.18$); however, the combination of tPA and AcSDKP administration significantly reduced the volumes with elevated permeability at 72h (30.1±16.7mm^3 vs 64.0±38.6mm^3, $p<0.04$) and 144h (18.3±9.8mm^3 vs 65.0±21.0mm^3, $p<0.001$) after stroke in rats, compared to tPA monotherapy. The mean K_i values of the volumes with elevated permeability were not significantly different at all three times of measurement between the two groups of rats (data not shown).

As shown in figure 3, T1WI images with Gd-DTPA enhancement from the same animals as in K_i maps (Fig.1), exhibited similar evolution patterns as the K_i maps. The quantitative data, in Fig.2b, of volumes with contrast enhancement in T1WI demonstrated approximately the same results as did K_i. Furthermore, the elevated K_i volumes were highly correlated ($R=0.82$, $p<10^{-4}$) with the Gd-DTPA enhanced volumes in T1WI images (Fig.4a), and mean K_i values in the measured volumes were highly correlated ($R=0.83$, $p<0.05$) with increased percentages of CE-T1WI image intensity (Fig.4b), measured at 6d after stroke.

The typical images from the representative rats are presented in figure 5 to demonstrate the evolution of ischemic lesion volumes after stroke. Starting with the approximate same size and location of ischemic lesion measured with ADC maps immediately after embolic MCAo (left column, Fig.5), the ischemic lesion volumes on T_2 maps (right columns, Fig.5) in the combination treated rat (upper row, Fig.5) were much smaller than the volumes in the 10 monotherapy rat (lower row, Fig.5) after stroke. Quantitative lesion volume measurements (Fig.2c) demonstrated that, no differences were detected on the ADC maps immediately after stroke and prior to the treatments between the two groups (64.2±10.1mm^3 vs 61.0±11.6mm^3, $p>0.54$); however, significant differences were found with T_2 maps acquired 3d and 6d after stroke between the two groups; for example, the ischemic lesion volumes were 113.6±24.9mm^3 for the combination treated rats and 188.1±60.8mm^3 for the monotherapy rats 6d after stroke ($p<0.04$). The ratio of BBB disruption volume per infarction volume is 0.16±0.08 for the combination treated group, and 0.37±0.14 for the monotherapy group at 144 h after stroke.

Representative histological pictures are presented in figure 6. On the H&E staining sections, the ischemic lesion volumes were 146.7±35.9mm^3 for the combination treated rats and 199.3±60.4mm^3 for the monotherapy rats, with significant differences ($p<0.05$) between the two groups. Using fibrin stained section (Fig.6 A, C), the total fibrin leakage areas were 0.063±0.059mm^2 and 0.172±0.103mm^2 for combination treatment and monotherapy rats, respectively. The total fibrin leakage areas were significantly reduced in the combination treatment rats, compared to the monotherapy rats ($p<0.03$). With the H&E staining, erythrocyte presence in brain parenchyma (Fig.6 B, D) was measured. The total area containing erythrocytes were 0.018±0.024mm^2 and 0.072±0.190mm^2 for combination treatment and monotherapy rats with MCID system, respectively. Although no significant difference was found between the two groups ($p>0.4$), the areas of parenchyma with erythrocyte appeared larger in the monotherapy rats than that in the combination treated rats.

The ischemic lesion volumes obtained from T_2 maps acquired 6 days after stroke were significantly correlated with the histological measurements of lesion volumes obtained from H&E staining ($R=0.67$, $p<0.003$). The total elevated K_i areas (derived from volumes) were also correlated with the fibrin leakage areas ($R=0.80$, $p<0.001$). Similarly, the total Gd-DTPA enhanced areas in T1WI images were significantly correlated with the fibrin leakage areas ($R=0.77$, $p<0.001$).

Discussion

The MRI permeability factor K_i is a measurement of the blood-to-brain transfer constant, and provides the rate of Gd-DTPA influx. The elevated K_i values indicate BBB damage leading to Gd-DTPA leakage (Ewing et al., 2006). In this study, K_i directly and noninvasively tracks the changes of BBB disruption before and after receiving the thrombolytic treatment in vivo for every animal, and provides more precise and reliable results than the traditional histological results, obtained in non-MRI studies by sacrificing different animals at different times. As a result, our K_i measurements demonstrate that the combination treatment, compared to tPA monotherapy, significantly reduces the volumes of the elevated K_i values at 3d and 6d after stroke, which indicates that the combination treatment significantly reduces the BBB disruption in embolic stroke rats. Furthermore, we found that the K_i results of BBB disruption were consistent and significantly correlated ($R=0.80$, $p<0.001$) with fibrin deposition in parenchymal tissue, measured at 6 days after embolism.

Gd-DTPA leakage is a hallmark of BBB disruption (Lo et al., 1994). With a molecular weight of approximate 1KDa, Gd-DTPA cannot cross the intact BBB. However, disruption of the BBB allows accumulation of Gd-DTPA in brain parenchyma, which primarily decreases the T_1 constant of cerebral tissue where it accumulates, leading to the increase of K_i values. Therefore, the elevated K_i values reflect the BBB disruption and relate to T1WI enhancement. Obviously, the evaluation of BBB disruption using MRI permeability measurements depends on the size of contrast agent used in the experiment. The intact BBB complex consists of endothelium, bounded by the basal lamina, and is encompassed by the end-feet of astrocytes. BBB damage after ischemia starts from breakdown of basal lamina with loss of astrocyte and endothelial cell contact, and subsequent increase of permeability to small molecules, such as Gd- DTPA, at an early stage after stroke, and for cells (e.g. fibrin and erythrocytes) in later times (Haring et al., 1996). The loss of basal lamina structure with breakdown of the extracellular matrix is the necessary step for the extravasation of plasma, and at later times blood components, into the brain parenchyma (Hamann et al., 1996). Therefore, the correlation of the MRI K_i evaluation with the histological measurements for BBB leakage strongly depends on the contrast agent used in MRI and the molecular or cellular size of leaked plasma or blood components inspected in histology. Thus, the histological fibrin measurements for the evaluation of BBB disruption should have a much higher correlation with MRI K_i measurements with Gd-DTPA than do erythrocyte measurements, since fibrinogen has a molecular weight of 340KDa and the fibrin dimer is 45nm in length (Walker and Nesheim, 1999, Chernysh and Weisel, 2008), much smaller than erythrocyte with 6~8μm in diameter.

The point of view above coincides with results of this study. No significant differences were found on histological measurements of erythrocytes in brain parenchyma between the combination treatment and the tPA monotherapy rats ($p>0.4$), although total areas of erythrocyte evidence in brain parenchyma were much smaller in the combination group than in the monotherapy group ($0.018\pm0.024mm^2$ vs $0.072\pm0.190mm^2$). One reason may be the stroke model in the study. There is an approximate 20% incidence of gross hemorrhage within 168 hours from the ischemia onset without any treatment in this embolic stroke model of rat (Zhang et al., 1997), and approximately 40% of rats treated with tPA alone at 4 hours post MCAo exhibit gross hemorrhage within 48 hours after stroke (Ding et al., 2005). The gross hemorrhage, comparable with symptomatic hemorrhage in the clinic, is defined as blood evident to the unaided eye on the H&E stained sections and confirmed by microscopy. According to the power (0.85) calculation, populations of experiment groups must be increase more than ten times the present number to achieve a meaningful statistical difference for the evaluation of gross hemorrhage.

The permeability K_i and CE-T1WI measurements are related (Ding et al., 2006). The present experiment demonstrated that both volume ($R=0.82$, $p<10^{-4}$) and mean ($R=0.83$, $p<0.05$) measurements of K_i, obtained immediately after Gd-DTPA injection, and CE-T1WI, acquired 25 minutes after Gd-DTPA injection for the post-Gd T1WI, were highly correlated (Fig.4). Like K_i, volumes measured by CE-T1WI for BBB disruption were significantly correlated with histological measurements of fibrin leakage areas ($R=0.77$, $p<0.001$). Hence, substituting CET1WI for permeability K_i measurements may be considered, if necessary, since CE-T1WI takes much less MRI acquisition and image post processing time.

In addition, the present MRI study has demonstrated that the combination treatment with tPA intravenously and with AcSDKP subcutaneously infused at a dose of 0.4mg/kg, at 4 hours of embolic stroke in rats, significantly reduced the ischemic lesion volumes at 3d and 6d after stroke, compared with tPA monotherapy, with the MRI results confirmed by the histological measurements. Our results, thus, indicate that the combination treatment of tPA and AcSDKP initiated at 4h after embolic MCAo is a neuroprotective treatment, which is consistent with our previous report (Zhang et al., 2014).

Cerebral ischemia upregulates tissue factor and matrix metalloproteinase (MMP) expression in endothelial cells (Lo et al., 2002), which facilitates inflammation and BBB disruption (Rosell and Lo, 2008). Treatment with tPA after stroke significantly increases cerebral microvascular MMP immunoreactivity (Zhang et al., 1999, Lo et al., 2002, Rosell and Lo, 2008); thus, delayed thrombolysis with tPA exacerbates the disruption of the vascular integrity and intracerebral hemorrhage after stroke (Lo et al., 2002), which limits the clinical use of tPA. Following the ischemic insult, toll-like receptors (TLRs) induce the expression of genes encoding for inflammation and apoptosis via nuclear transcription factor κB (NF-κB) (Caso et al., 2007). In addition, elevation of plasminogen activator inhibitor-1 (PAI-1) activity is included in the coagulation cascades after ischemia (Zhang et al., 1999). Activation of transforming growth factor β1 (TGF β 1) upregulates PAI-1 (Datta et al., 2000), which contributes to intravascular fibrin deposition after onset of focal embolic ischemia and directly obstructs cerebral microcirculation (Zhang et al., 1999). However,

previous studies showed that AcSDKP treatment protects against renal and cardiac damage via inhibiting TGFβ1 and NF-κB mediated inflammatory response and fibrosis (Rhaleb et al., 2013). Thus, the adjuvant AcSDKP in tPA treatment of embolic stroke, via TLRs/NF-κB and TGFβ1/PAI-1 pathways, may play an important role in regulating inflammation and thrombosis responses after stroke, leading to a neuroprotective effect of tPA administered at 4 hours post onset of MCAo and a decrease of BBB disruption after embolic stroke.

Conclusions

The combination treatment of embolic stroke in rats with tPA and AcSDKP initiated at 4 hours after onset of MCAo significantly reduced the volume of BBB disruption measured in vivo at 72 and 144 hours after stroke by MRI, which was confirmed by ex vivo measurements with immunohistochemical stains, compared to tPA monotherapy. The reduced BBB disruption may be associated with lower hemorragic risk after receiving thrombolytic treatment with tPA. MRI permeability K_i, as well as CE-T1WI, measurements for BBB disruption were consistent and highly correlated with histological measurements of fibrin antigen. These data suggest that AcSDKP likely acts on the neurovascular unit to enhance BBB integrity and exert the neuroprotective effect observed in the combination therapy.

Acknowledgments

This work was financially supported by NIH RO1 NS079612 (ZZ), RO1 NS064134 (QJ) and RO1 AG037506 (MC). The content is solely the responsibility of the authors and does not necessarily represent the official view of the National Institutes of Health.

Abbreviations

AcSDKP	N-acetyl-seryl-aspartyl-lysyl-proline
ADC	apparent diffusion coefficient
ANOVA	analysis of variance
BBB	blood-brain barrier
CE-T1WI	contrast enhanced T_1-weighted imaging
DWI	diffusion-weighted imaging
Gd-DTPA	gadolinium-diethylenetriamine penta-acetic acid
H&E	hematoxylin and eosin
L-L	Look-Locker
MCA	middle cerebral artery
MCAo	middle cerebral artery occlusion
MCID	MicroComputer Imaging Device
MMP	matrix metalloproteinase
MRI	magnetic resonance imaging

NF-κB	nuclear transcription factor κB
PAI-1	plasminogen activator inhibitor-1
ROI	region-of-interest
SD	standard deviation
T2WI	T_2-weighted imaging
TGFβ1	transforming growth factor β1
TLRs	toll-like receptors
tPA	tissue plasminogen activator.

Reference

Caso JR, Pradillo JM, Hurtado O, Lorenzo P, Moro MA, Lizasoain I. Toll-like receptor 4 is involved in brain damage and inflammation after experimental stroke. Circulation. 2007; 115:1599–1608. [PubMed: 17372179]

Chernysh IN, Weisel JW. Dynamic imaging of fibrin network formation correlated with other measures of polymerization. Blood. 2008; 111:4854–4861. [PubMed: 18272815]

Datta PK, Blake MC, Moses HL. Regulation of plasminogen activator inhibitor-1 expression by transforming growth factor-beta -induced physical and functional interactions between smads and Sp1. J Biol Chem. 2000; 275:40014–40019. [PubMed: 11054406]

Ding G, Jiang Q, Li L, Zhang L, Gang Zhang Z, Ledbetter KA, Ewing JR, Li Q, Chopp M. Detection of BBB disruption and hemorrhage by Gd-DTPA enhanced MRI after embolic stroke in rat. Brain Res. 2006; 1114:195–203. [PubMed: 16950236]

Ding G, Jiang Q, Zhang L, Zhang ZG, Li L, Knight RA, Ewing JR, Wang Y, Chopp M. Analysis of combined treatment of embolic stroke in rat with r-tPA and a GPIIb/IIIa inhibitor. J Cereb Blood Flow Metab. 2005; 25:87–97. [PubMed: 15678115]

Ewing JR, Brown SL, Lu M, Panda S, Ding G, Knight RA, Cao Y, Jiang Q, Nagaraja TN, Churchman JL, Fenstermacher JD. Model selection in magnetic resonance imaging measurements of vascular permeability: Gadomer in a 9L model of rat cerebral tumor. J Cereb Blood Flow Metab. 2006; 26:310–320. [PubMed: 16079791]

Fieschi C, Argentino C, Lenzi GL, Sacchetti ML, Toni D, Bozzao L. Clinical and instrumental evaluation of patients with ischemic stroke within the first six hours. J Neurol Sci. 1989; 91:311–321. [PubMed: 2671268]

Hacke W, Kaste M, Bluhmki E, Brozman M, Davalos A, Guidetti D, Larrue V, Lees KR, Medeghri Z, Machnig T, Schneider D, von Kummer R, Wahlgren N, Toni D. Thrombolysis with alteplase 3 to 4.5 hours after acute ischemic stroke. N Engl J Med. 2008; 359:1317–1329. [PubMed: 18815396]

Haelewyn B, Risso JJ, Abraini JH. Human recombinant tissue-plasminogen activator (alteplase): why not use the 'human' dose for stroke studies in rats? J Cereb Blood Flow Metab. 2010; 30:900–903. [PubMed: 20216551]

Hamann GF, Okada Y, del Zoppo GJ. Hemorrhagic transformation and microvascular integrity during focal cerebral ischemia/reperfusion. J Cereb Blood Flow Metab. 1996; 16:1373–1378. [PubMed: 8898714]

Haring HP, Berg EL, Tsurushita N, Tagaya M, del Zoppo GJ. E-selectin appears in nonischemic tissue during experimental focal cerebral ischemia. Stroke. 1996; 27:1386–1391. discussion 1391–1382. [PubMed: 8711807]

Jackson JD, Ozerol E, Yan Y, Ewel C, Talmadge JE. Activity of acetyl-Ser-Asp-Lys-Pro (AcSDKP) on human hematopoietic progenitor cells in short-term and long-term bone marrow cultures. J Hematother Stem Cell Res. 2000; 9:489–496. [PubMed: 10982247]

Liu JM, Lawrence F, Kovacevic M, Bignon J, Papadimitriou E, Lallemand JY, Katsoris P, Potier P, Fromes Y, Wdzieczak-Bakala J. The tetrapeptide AcSDKP, an inhibitor of primitive hematopoietic cell proliferation, induces angiogenesis in vitro and in vivo. Blood. 2003; 101:3014–3020. [PubMed: 12480715]

Lo EH, Pan Y, Matsumoto K, Kowall NW. Blood-brain barrier disruption in experimental focal ischemia: comparison between in vivo MRI and immunocytochemistry. Magn Reson Imaging. 1994; 12:403–411. [PubMed: 8007769]

Lo EH, Wang X, Cuzner ML. Extracellular proteolysis in brain injury and inflammation: role for plasminogen activators and matrix metalloproteinases. J Neurosci Res. 2002; 69:1–9. [PubMed: 12111810]

NINDS. Intracerebral hemorrhage after intravenous t-PA therapy for ischemic stroke. The NINDS t-PA Stroke Study Group. Stroke. 1997; 28:2109–2118. [PubMed: 9368550]

Rasoul S, Carretero OA, Peng H, Cavasin MA, Zhuo J, Sanchez-Mendoza A, Brigstock DR, Rhaleb NE. Antifibrotic effect of Ac-SDKP and angiotensin-converting enzyme inhibition in hypertension. J Hypertens. 2004; 22:593–603. [PubMed: 15076166]

Rhaleb NE, Pokharel S, Sharma UC, Peng H, Peterson E, Harding P, Yang XP, Carretero OA. N-acetyl-Ser-Asp-Lys-Pro inhibits interleukin-1beta-mediated matrix metalloproteinase activation in cardiac fibroblasts. Pflugers Arch. 2013; 465:1487–1495. [PubMed: 23652767]

Rosell A, Lo EH. Multiphasic roles for matrix metalloproteinases after stroke. Curr Opin Pharmacol. 2008; 8:82–89. [PubMed: 18226583]

Walker JB, Nesheim ME. The molecular weights, mass distribution, chain composition, and structure of soluble fibrin degradation products released from a fibrin clot perfused with plasmin. J Biol Chem. 1999; 274:5201–5212. [PubMed: 9988770]

Wang D, Carretero OA, Yang XY, Rhaleb NE, Liu YH, Liao TD, Yang XP. N-acetylseryl- aspartyl-lysyl-proline stimulates angiogenesis in vitro and in vivo. Am J Physiol Heart Circ Physiol. 2004; 287:H2099–H2105. [PubMed: 15256375]

Yang F, Yang XP, Liu YH, Xu J, Cingolani O, Rhaleb NE, Carretero OA. Ac-SDKP reverses inflammation and fibrosis in rats with heart failure after myocardial infarction. Hypertension. 2004; 43:229–236. [PubMed: 14691195]

Zhang L, Chopp M, Teng H, Ding G, Jiang Q, Yang XP, Rhaleb NE, Zhang ZG. Combination treatment with AcSDKP and tissue plasminogen activator provides potent neuroprotection in rats after stroke. Stroke. 2014 (in press).

Zhang L, Zhang ZG, Chopp M. The neurovascular unit and combination treatment strategies for stroke. Trends Pharmacol Sci. 2012; 33:415–422. [PubMed: 22595494]

Zhang RL, Chopp M, Zhang ZG, Jiang Q, Ewing JR. A rat model of focal embolic cerebral ischemia. Brain Res. 1997; 766:83–92. [PubMed: 9359590]

Zhang ZG, Chopp M, Goussev A, Lu D, Morris D, Tsang W, Powers C, Ho KL. Cerebral microvascular obstruction by fibrin is associated with upregulation of PAI-1 acutely after onset of focal embolic ischemia in rats. J Neurosci. 1999; 19:10898–10907. [PubMed: 10594071]

Zhuo JL, Carretero OA, Peng H, Li XC, Regoli D, Neugebauer W, Rhaleb NE. Characterization and localization of Ac-SDKP receptor binding sites using 125I-labeled Hpp-Aca-SDKP in rat cardiac fibroblasts. Am J Physiol Heart Circ Physiol. 2007; 292:H984–H993. [PubMed: 17028162]

1. Treatment of stroke with tPA and AcSDKP reduced the volume of BBB disruption.
2. MRI permeability result for BBB correlated with measurements of fibrin antigen.
3. AcSDKP enhanced BBB integrity and exert the neuroprotective effect.
4. The reduced BBB disruption may be associated with lower hemorragic risk.

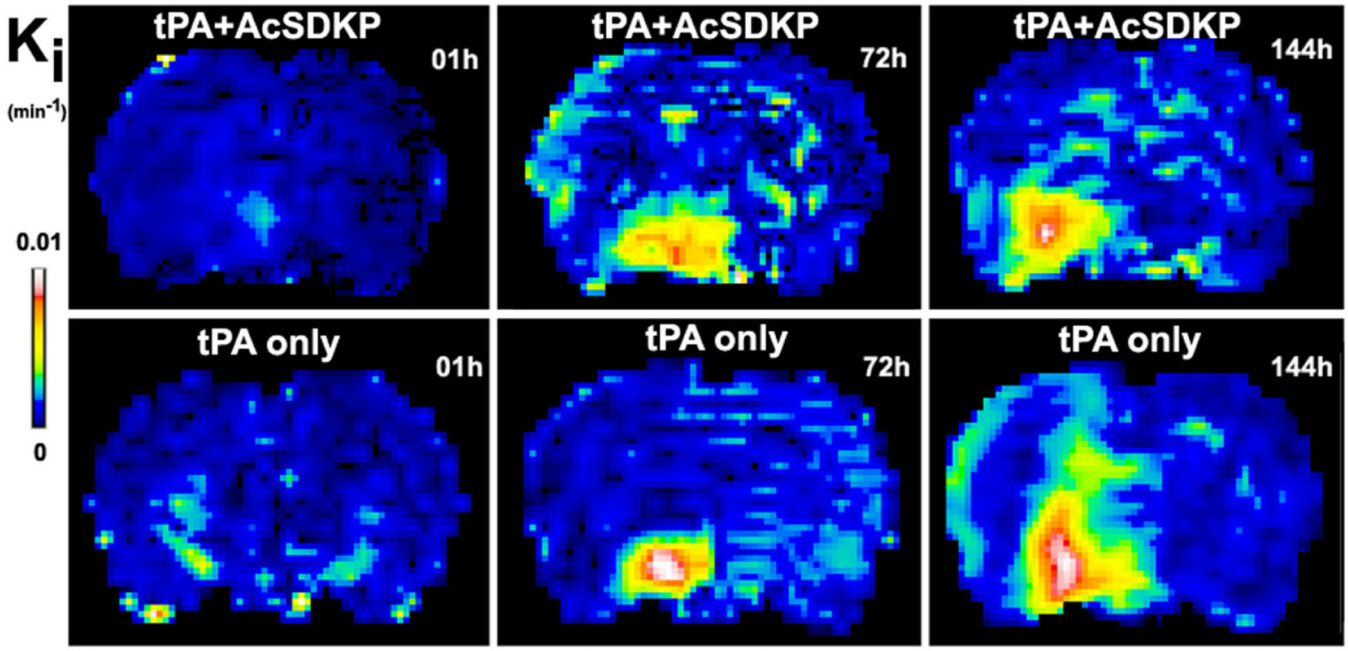

Figure 1.

The typical evolution patterns of K_i, which detected BBB disruption at 1h, 72h and 144h after ischemic stroke, are demonstrated for a representative rat treated with tPA and AcSDKP (upper row) or tPA alone (lower row), respectively. The volume with elevated permeability values increased more slowly in the rat administered with tPA and AcSDKP than in the rat with tPA monotherapy.

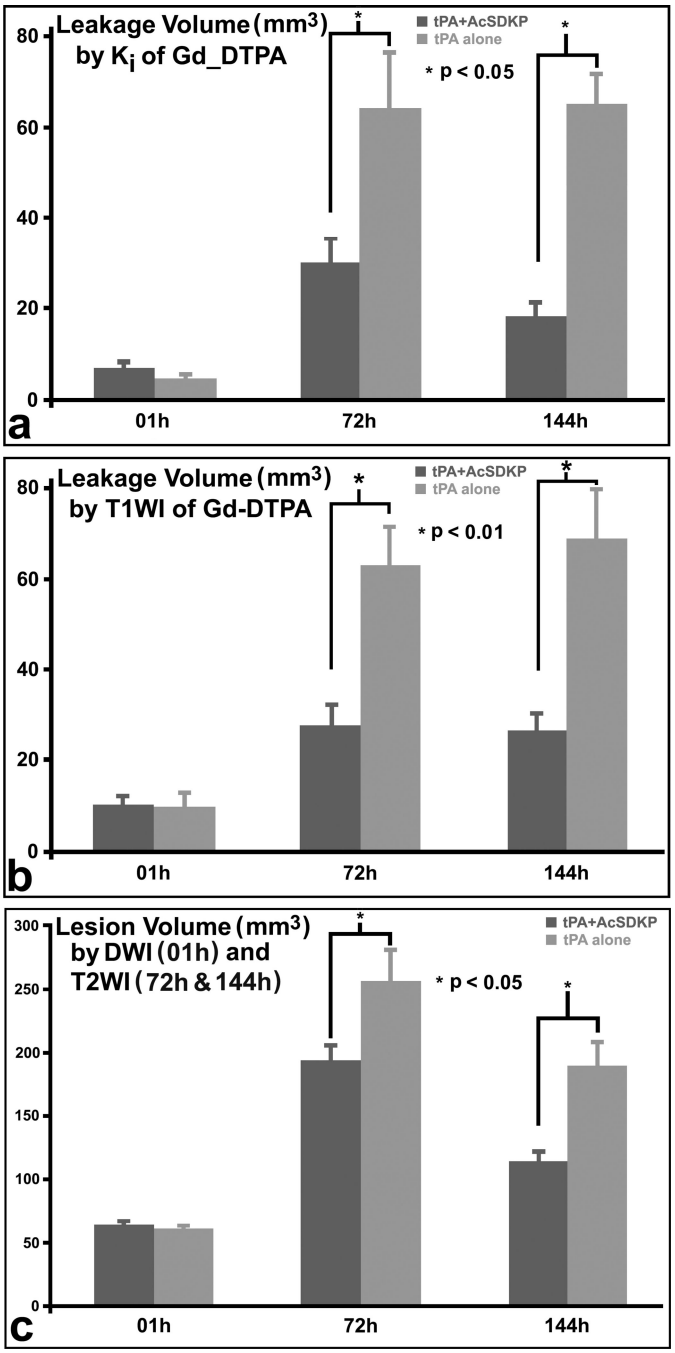

Figure 2.

The MRI quantitative measurements demonstrated that the tPA and AcSDKP treatment significantly ($p<0.05$) reduced both BBB disruption volumes measured by K_i (a) or CE-T1WI (b), and ischemic lesion volumes by T2WI (c), at 72h and 144h after stroke in rats, compared to tPA monotherapy.

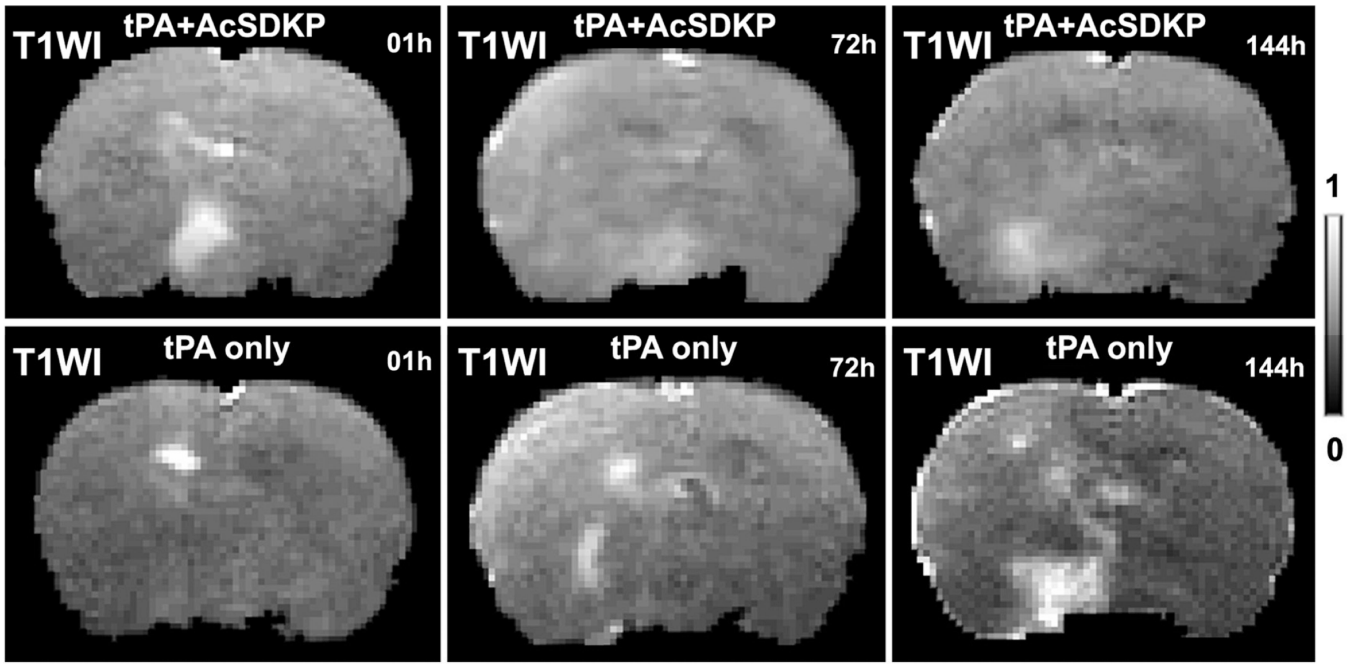

Figure 3.

The T1WI images acquired after Gd-DTPA injection exhibited smaller enhanced volumes in the representative rat treated with tPA and AcSDKP (upper row) than in the rat with tPA monotherapy (lower row).

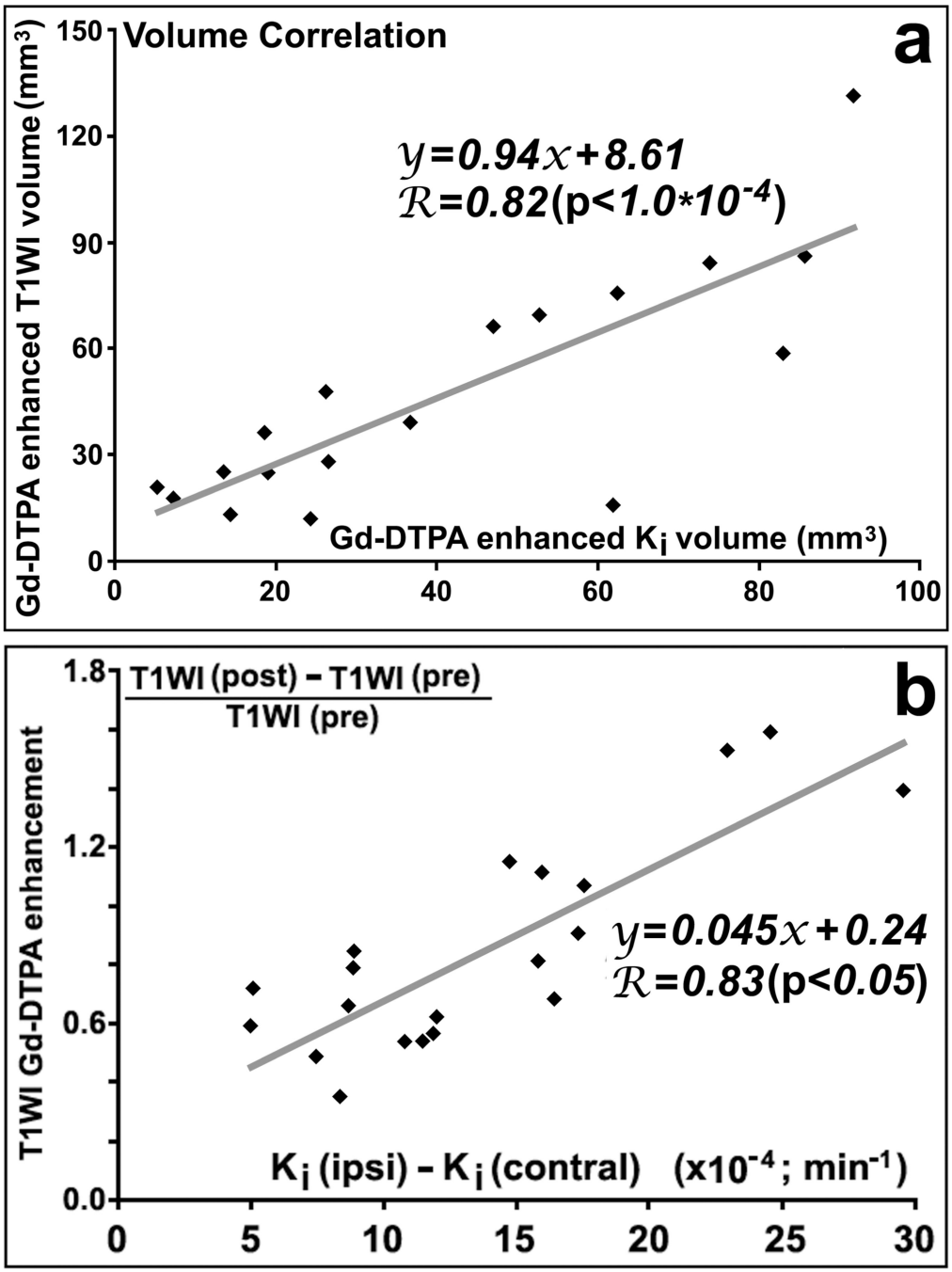

Figure 4.

Both Gd-DTPA enhanced volumes (R=0.82, $p<10^{-4}$; a) and mean values in the volume (R=0.83, p<0.05; b) measured by permeability K_i and CET1WI of Gd-DTPA were highly correlated at 6d after stroke in rats, respectively.

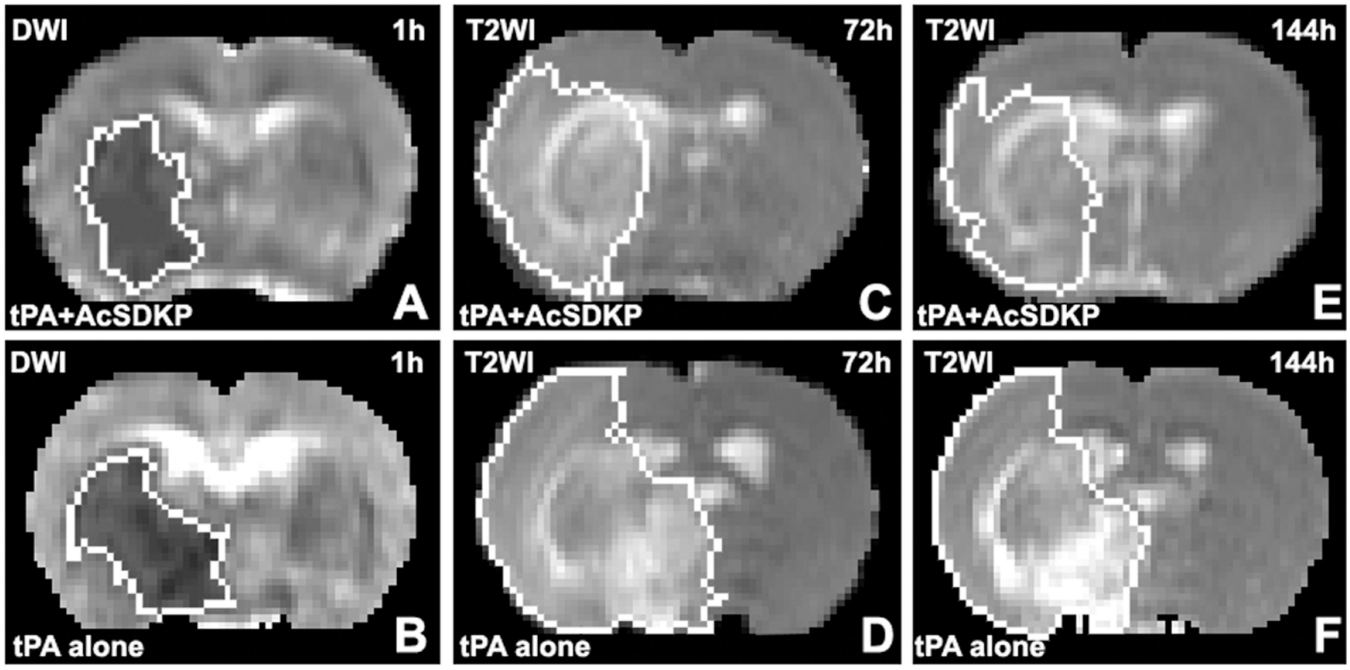

Figure 5.

Starting with approximately the same size and location of ischemic lesion measured by ADC maps immediately after embolic MCAo (left column), T_2 maps (right two columns) in the rat treated with tPA and AcSDKP (upper row) exhibited much smaller lesion volumes than the rat treated with tPA alone (lower row) at 3 and 6 days after stroke.

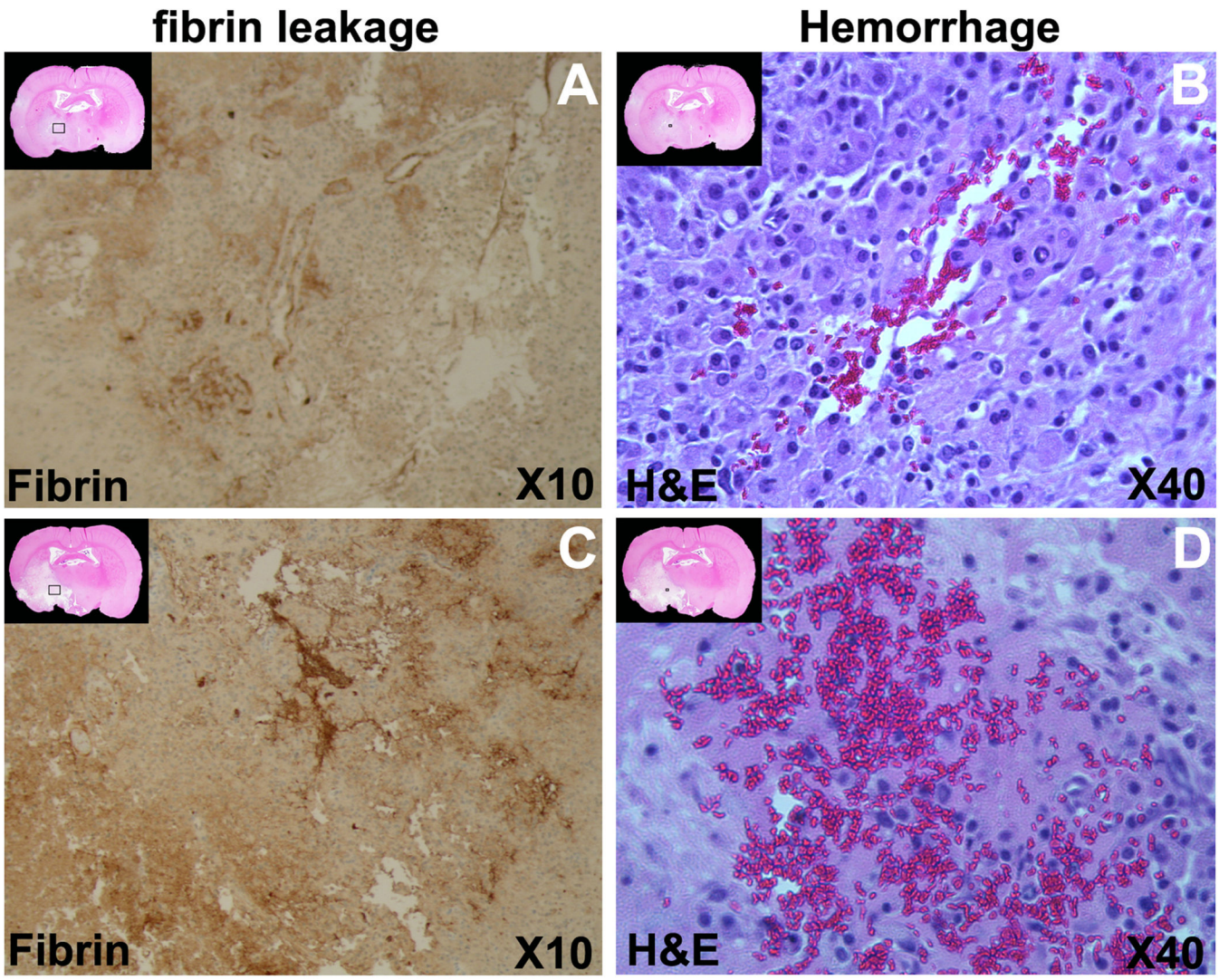

Figure 6.

The immunohistochemical staining slices are presented for the representative combination treated rat and the tPA monotherapy rat. The reduced H&E staining images at up-left corner of each panels display the locations for the corresponding immunohistochemical staining slices. The fibrin antigen stained slices demonstrated that the fibrin leakage was less severe in the rat receiving combination treatment (A) than tPA monotherapy (C). Areas containing erythrocytes in brain parenchyma were much smaller in the combination treated rat (B), than in the tPA monotherapy rat (D).

Table 1

BBB disruption volume (mm^3) measure by K_i map

Treatment	Rat	01h	72h	144h
tPA with AcSDKP	T1	5.03	4.78	7.09
	T2	3.13	22.38	26.03
	T3	6.44	55.38	24.38
	T4	0.00	52.75	36.63
	T5	7.31	41.03	18.88
	T6	13.69	29.31	5.13
	T7	12.06	27.25	14.19
	T8	4.25	22.66	18.56
	T9	9.44	15.75	13.34
tPA alone	C1	8.38	11.63	26.63
	C2	0.00	119.81	85.56
	C3	5.63	105.25	61.81
	C4	6.06	39.00	52.56
	C5	0.00	14.81	91.88
	C6	0.00	45.31	62.38
	C7	5.06	69.13	46.94
	C8	5.63	87.56	73.81
	C9	7.50	83.19	83.00